



Spatiotemporal monitoring of post-fire soil erosion rates using earth observation (EO) data and cloud computing

Stefanos P. Stefanidis¹ · Nikolaos D. Proutsos² · Alexandra D. Solomou² · Panagiotis Michopoulos² · Athanassios Bourletsikas² · Dimitris Tigkas³ · Velibor Spalevic⁴ · Shuraik Kader⁵

Received: 30 May 2024 / Accepted: 29 August 2024
© The Author(s), under exclusive licence to Springer Nature B.V. 2024

Abstract

This research addressed on the crucial concern of soil erosion in the post-fire Mediterranean landscapes, regarding disastrous wildfires in Greece during 2021. These fires broke out at the Varympompi, Schinos, and Ancient Olympia-Gortynia. To accomplish these goals, the Revised Universal Soil Loss Equation (RUSLE) and Earth Observation (EO) data coupled with Google Earth Engine (GEE) were used to quantify the wildfire effects on erosion dynamics in the burned areas as well as the regulation provided from the emergency post-fire rehabilitation treatments. High-resolution EO data such as Sentinel-2 imagery and climate data from ERA5-Land were processed over the GEE platform to assess soil erosion factor changes before and after the fire occurrence. The analysis was followed up by measurements of the vegetation recovery and rainfall erosivity, which are crucial for the knowledge of erosion processes in such regions. Results displayed great increases in soil erosion post-fire, with rates at Ancient Olympia-Gortynia rising to $118.3 \text{ t ha}^{-1} \text{ y}^{-1}$ in the first hydrological year after fire from pre-fire rates of $9.8 \text{ t ha}^{-1} \text{ y}^{-1}$. At Schinos site, rates increased from a pre-fire average of 11.6 to $72.2 \text{ t ha}^{-1} \text{ y}^{-1}$, and in Varympompi, from 4.8 to $28.8 \text{ t ha}^{-1} \text{ y}^{-1}$. Post-fire restoration works reduced erosion processes by approximately 18%. Coupling RUSLE with GEE offers a novel opportunity for dynamic monitoring of soil erosion towards informing land management and policy formulation in the fire-prone Mediterranean ecosystems in relation to the mitigation of erosion. The policy formulation on land management within fire-prone Mediterranean-type ecosystems stands to be influenced by the findings of the current study. Indeed, this is of worldwide importance, whereby management practices need to be adopted to ensure that ecosystems recover rapidly and effectively after fires for the conservation of soil resources.

Keywords RUSLE · Wildfires · Mediterranean landscape · Vegetation recovery · Sentinel-2; Era5-land; restoration works

1 Introduction

Fire, arguably one of the strongest ecological agents (Bond et al. 2005; Pausas and Ribeiro 2017), is a key determinant in the composition of plant communities in the world's terrestrial ecosystems. Evidence from the Mediterranean basin is that the fires have occurred during the late Quaternary time, extending much earlier ages as demonstrated by (Carrión et al. 2003). Many species have developed adaptive mechanisms to persist and regenerate after recurrent fires, justifying that wildfires are part and parcel of Mediterranean ecosystems (Spanos et al. 2000; Pausas et al. 2004). Since fires in the Mediterranean basin are a natural phenomenon that has gone on for millions of years has resulted in the development of adaptive mechanisms by plants. Wildfires have been major architects for shaping the Mediterranean landscapes in current mosaic-like patterns with levels of regeneration and degradation varied in space. With this context in mind, fires should not be treated as ecological disasters but seen as part of the natural process (Pausas et al. 2008). However, ecological disasters have taken place since ancient Greece when fires, grazing and erosion happened in successional steps. The philosopher Plato described the Greek mountains that suffered these steps as the bones of a diseased person.

The Mediterranean region in the Southern Europe is with hot and long dry summers, together with vegetation, which is flammable, and complex terrain favoring wildfire initiation and spread, adds to human activities. In fact, the population of Southern Europe has increased over the last decades, and gradually the wildland–urban interface (WUI), that is, the distance between housing and forested areas, decreases (Mitsopoulos et al. 2020). The problem of wildfires is a major issue for the entire region. More specifically, the anthropogenic pressure on natural ecosystems, in addition to its contribution to the climate crisis, has lately increased both the number of wildfires and the affected areas, and, consequently, the socio-economic and environmental impacts (Vilar et al. 2016; Pausas and Keeley 2021). To that end, the scientific community has paid attention to the footprint of the wildfires on ecosystem services (Lecina-Diaz et al. 2021; Silvestro et al. 2021). Studies have shown the increased susceptibility to erosion in post-fire scenarios, highlighting the importance of effective monitoring and management strategies (Valkanou et al. 2022).

Important changes in the hydrological and erosion regimes under post-wildfire conditions arise from the depletion of vegetation, transformed properties of the soil, and increased runoff (Shakesby and Doerr 2006; Moody et al. 2013; Akin et al. 2023). These favorable conditions further add to the detachment and transportation of soil particles, especially under rainy conditions, which further lead to the continuous deterioration of soil through the process of accelerated erosion in the areas affected by fires. In addition, the micrometeorological, hydraulic, physical and chemical properties of the ecosystems are greatly affected (Proutsos et al. 2023; Michopoulos et al. 2023; Solomou et al. 2023; Bashir et al. 2024a). The soil loss through fire is a process that involves many factors: the most important ones are burning severity, slope, texture of the soil, and composition, among others. An additional imperative factor is the pre-fire weather effect. In the aftermath of wildfires, a key priority is the protection of forest soils, which underlines the crucial need for erosion control. In this respect, post-fire, site-specific restoration works have the double task of avoiding land degradation and allowing natural regeneration on the one side and conveying information on the effective quantification of soil erosion in post-wildfire scenarios on the other hand (Girona-García et al. 2021; Bombino et al. 2023). The assessment and management of natural and technological hazards are crucial for sustainable development emphasize the need for integrated planning solutions (Skilodimou and Bathrellos

2021). Certainly, a clear, quantitative characterization of soil erosion in burned areas is of paramount importance for the delivery of information to policymakers regarding the magnitude of the post-fire associated erosion risk; it is also valuable in designing and implementing targeted mitigation measures, including urgent hillslope recovery actions and thorough watershed stabilization plans (Myronidis and Arabatzis 2009; Robichaud & Ashmun 2012).

Numerous scholars have investigated post-fire erosion using both empirical models (Karamesouti et al. 2016; Mallinis et al. 2016; Lanorte et al. 2019; Efthimiou et al. 2020a) and field measurements (Stefanidis et al. 2002; Robichaud 2005; Spiegel and Robichaud 2007). While direct measurements serve as crucial ground truth data for calibrating and verifying models, systematic field measurements are prohibitively expensive, requiring increased human and technological resources. Additionally, field plots are usually limited to selected sites and, therefore, results from this survey method do not sufficiently cover fire-affected areas. Measurements are not systematic but carried out for a limited period, so the results are representative of the local conditions, and this hampers extrapolation to larger scales and different environments (Vanmaercke et al. 2012; Bashir et al. 2024b). The integration of GIS and remote sensing (RS) technologies provides a powerful tool for assessing and mapping soil erosion susceptibility, as demonstrated in various studies (Islam et al. 2022). Despite inherent uncertainties in predicting erosion with empirical models (Lopes et al. 2021), their widespread application is attributed to their straightforward design and minimal data needs, enabling large-scale quantitative monitoring of soil loss rates.

The USLE model proposed in 1978 by Wischmeier & Smith and its modification RUSLE by Renard et al. in 1991, are among the widely used experimental models for erosion estimation (Sestras et al. 2023). The (R) USLE help provide spatially distributed estimates over vast areas. For this reason, the success of this type of model lies in its low demands in terms of data availability and simplicity of interpretation, while offering uncertainty levels comparable to much more complex models that are also demonstrate global transferability (Alewell et al. 2019; Bammou et al. 2024a; Sadkaoui et al. 2024). Accordingly, the revised modeling application approach has been very well applied to the entire Mediterranean region, demonstrating enhanced efficiency in the calculation of soil loss rates (Efthimiou 2016; Duarte et al. 2021). Since the RUSLE describes a low number of parameters, and with new possibilities emerging from the already existing availability of Earth Observation (EO) sensor data, the update is presented for the spatial determination of these parameters. This feature makes this model suitable for dynamically monitoring erosion processes at different scales (Alewell et al. 2019). The advent of cloud processing systems including GEE, which offers free worldwide access to the EO datasets (Gorelick et al. 2017), has showed great potential for monitoring the changes in erosion rates (Wang and Zhao, 2020; Brovelli et al. 2020). To that end, integrating the RUSLE model with GEE capabilities makes it powerful in quantifying how land cover changes affect erosion across many geographical and temporal scales (Stefanidis et al. 2022; Demir and Dursun 2024; Nourizadeh et al. 2024).

This study aims to evaluate the spatiotemporal changes in soil erosion rates and their driving factors by quantifying the combined impacts on post-fire erosion dynamics in the case of the most recent large-scale 2021 destructive wildfires in Greece. Open-access EO data were utilized with cloud computing to determine more detailed monitoring of the processes of soil erosion using the RUSLE model. Specific objectives include: (i) the estimation vegetation recovery effects on erosion rates and (ii) the quantification of erosion regulation service provided by the emergency post—fire restoration works. Employing the

RUSLE model with open-access EO data and cloud computing ensures meticulous monitoring of processes of soil erosion. By enforcing the need for strategic interventions, this study contributes to the deeper comprehension of post-fire erosion impact and its mitigation, informing sustainable land management and restoration strategies.

2 Materials and methods

2.1 Study area

The research was conducted in specific Greek regions that were severely affected by the megafires in 2021. More specifically, three characteristic sites were chosen for detailed study: Varympompi in Attica, Schinos in Corinthia, and Ancient Olympia and Gortynia in Iliia. Burned expenses in these regions total more than 5,000 hectares and are of primary interest because of their strategic proximity to important urban centres, tourist attractions, and archaeological sites. Under this rationale, the social importance of these areas and their high value in the wider framework are justified by the fact of the presence of effective post-fire management and full erosion monitoring at the same time. At the same time, the selection of the present sites will provide a representative spatial distribution all over the Greek territory, in support of holistic examination of the post-fire landscape and erosion dynamics and challenges related to the management.

In Varympompi, the dominant type of forest vegetation was transitional forested and shrubby areas (24.3%), while significantly increased were the coverage of mixed forest (21.9%), agricultural areas (21.2%), and coniferous forest (15.4%). In Schinos, the dominant coverage type was coniferous forest (64.3%) and in Ancient Olympia—Gortynia, the dominant types of forest vegetation were transitional forested and shrubby areas (13.1%), mixed forest (12.3%), hard-leaved vegetation (8.5%), and, secondarily, coniferous forest (2.6%), as depicted from the Corine CLC 2018, land cover product. *Poaceae*, *Asteraceae*, *Fabaceae*, *Cistaceae*, and *Rosaceae* are the most important families of plant species in the three regions in the postfire environment based on in-situ floristic recordings implemented during the years 2022 and 2023 (Solomou et al. 2023).

Based on data from the nearest long operating meteorological stations of the Hellenic National Meteorological Service (Corinth: 37.93° N, 22.95° E, Alt. 14 m; Tatoi-Attica: 38.10° N, 23.78° E, Alt. 236 m; Pyrgos-Iliia: 37.67° N, 21.43° E, Alt.: 13 m), the climate varies between the burnt areas. Specifically, Varympompi and Schinos are characterized by a semi-humid climate. Still, Ancient Olympia's climate is humid, according to UNEP's (1992) aridity classification system, which is based on Thornthwaite's (1948) water balance approach (Tsiros et al. 2020; Proutsos et al. 2021, 2022). It should also be noted that the semi-arid areas present a change to more arid conditions, compared to the past, whereas the humid ones are becoming wetter (Tsiros et al. 2020; Proutsos et al. 2022). Figure 1 illustrates the locations of the fire-affected sites.

The burned areas were estimated through the Copernicus Emergency Management Service (EMS), available from the following link: <https://emergency.copernicus.eu/mapping/list-of-activations-rapid>. This service provides rapid, on-demand geospatial information to support emergency management. Such information is normally made available within hours to support the emergency management community in the immediate aftermath of a disaster. The service quickly accessed, processed, and analyses satellite products and other

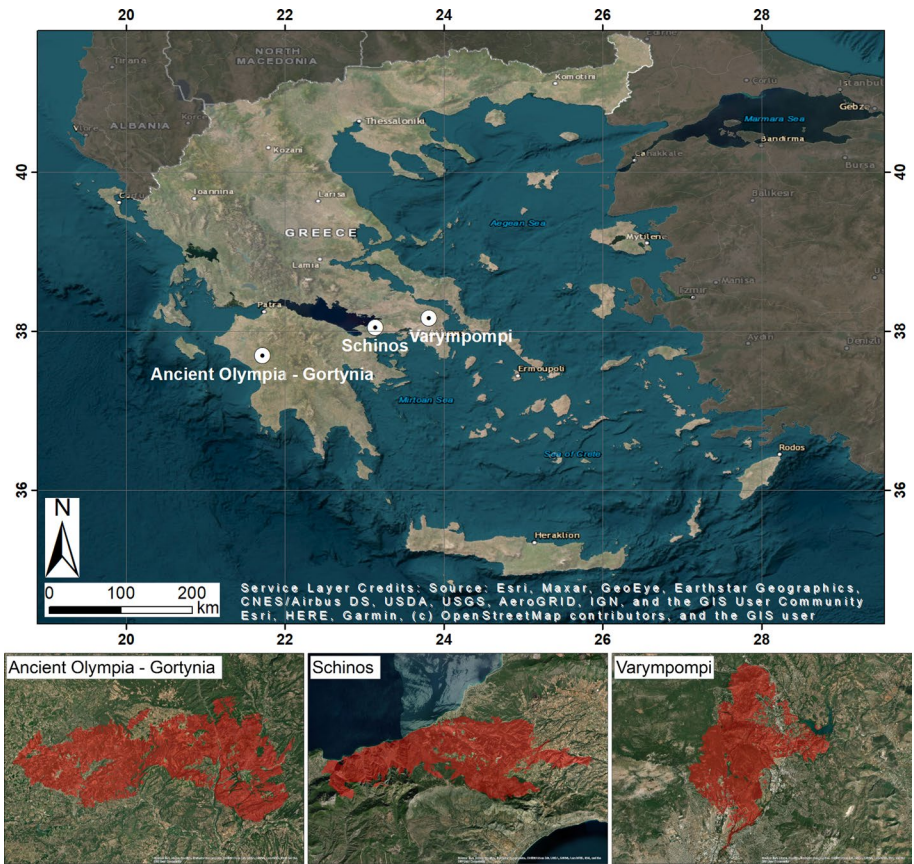


Fig. 1 Location of fire-affected sites (white points) and corresponding burned areas (red polygon) in Greece

geospatial datasets. In Table 1, the analytical information on the start date and the extent of burned areas in hectares is shown.

2.2 Data acquisition and pre-processing

To fulfill the objectives of the current study, various EO datasets were acquired and processed. They included satellite images, topographic and pedological data, climatic

Table 1 Attributes of wildfire incidents from copernicus EMS

Site	Starting date	EMS activation code	Hectares of burned area
Ancient Olympia—Gortynia (Iliia)	4/8/2021	EMRS528	18,400
Schinos (West Attica—Corinthia)	19/5/2021	EMRS510	7,005
Varympompi (Attica)	3/8/2021	EMRS527	8,454

information, and land management taken from accessible open databases. The GEE cloud platform is utilized to provide multiple available datasets under its dependable and high-powered cloud infrastructure. (Elnashar et al. 2021). GEE is widely used since it provides effective solutions for handling and processing data on powerful servers. Introduced by Google in 2010, GEE offers access to EO datasets via its online Python APIs and a web-based JavaScript Interactive Development Environment (IDE). The substantial volume of accessible data, coupled with the substantial processing capabilities, positions GEE as an efficient and powerful tool for environmental monitoring (Tamiminia et al. 2020). All datasets were organized into GIS thematic layers utilizing the free and open-source QGIS (v3.22) software.

Sentinel-2 optical data (S2), obtained at Level 2A (L2A) from the European Space Agency (ESA) via the GEE catalogue, were utilized in this study. The Sentinel-2 satellites are outfitted with the MSI multispectral optical sensor, which captures images in 13 different spectral bands with 10–60 m spatial resolution, revisited every five days. The L2A data provide a bottom-of-atmosphere (BOA) reflectance ortho-image product. The spatial and spectral characteristics of S2 imagery are crucial for identifying vegetation types and species and monitoring vegetation status (Immitzer et al. 2016, Verde et al. 2020). Following wildfires, many Sentinel-2 images, each with a cloud cover of less than 10%, were collected using the GEE platform to create a mosaic for the study areas within each hydrological year (October to September). Subsequently, all bands were resampled to a 10 m resolution. The pre-fire condition was determined by creating a mosaic of S2-L2A images spanning the three hydrological years preceding the wildfire event, in alignment with recommendations from existing literature (Vieira et al. 2023). This method leverages the wide coverage and high temporal resolution from the S2-L2A data to study vegetation dynamics and land surface attributes in detail and over a long period, in a very broad manner, to understand the state of a landscape before a wildfire.

Climatic data used in this research were derived from a monthly-accumulated precipitation aggregation time series of the developed reanalysis product from the European Center for Medium Range Weather Forecasts (ECMWF), ERA5-Land, via GEE. For the periods prior to the fire, the analysis covered the hydrological years 2017–2018, 2018–2019, 2019–2020. Subsequently, post-fire period data from the hydrological years 2021–2022 and 2022–2023 were examined. The spatial resolution of ERA5-Land data is approximately $0.1^\circ \times 0.1^\circ$ (~9 km). Previous studies (Alexandridis et al. 2023; Gomis-Cebolla et al. 2023) have demonstrated ERA5-Land's satisfactory performance in accurately reproducing precipitation accumulations and patterns in Mediterranean climates.

Soil properties were retrieved from the SoilGrids assets at a 250 m resolution. SoilGrids is a digital system for soil mapping, where machine learning techniques are applied to an international compilation of soil profiles and environmental information (Hengl et al. 2017). This valuable dataset, now accessible through GEE, includes information on the fractions of sand, clay and silt contents (%), organic matter content (%), and soil permeability and structure. The Forest and Buildings Removed DEM (FABDEM) was utilized to analyze the studied regions' topography. This global elevation model removes height distortions brought about by buildings and trees employing machine learning applied to data from the Copernicus GLO 30 Digital Elevation Model, amongst other improvements (Hawker et al. 2022). That makes FABDEM the obvious preferable choice, especially for regions with high vegetation, with obvious improvements over other DEM products. The academics, therefore, recommend that FABDEM be used in forested mountain catchments to underpin its use as a state-of-the-art data product for topographic analysis that is both precise and reliable (Marsh et al. 2023).

Table 2 Spatial datasets employed in the current research

Dataset	Data source	Data accessibility	Spatial resolution
Sentinel-2 (L2A)	ESA via GEE	ee.ImageCollection("COPERNICUS/S2_SR")	10 m
ERA5-Land	ECMWF via GEE	ee.ImageCollection("ECMWF/ERA5/DAILY")	~9 km
SoilGrids	ISRIC via GEE	ee.Image("projects/soil_grids-istic/layer_name")	250 m
FABDEM	Bristol's University	https://data.bris.ac.uk/data/dataset/s5hqmjcdj8yo2ibz79b4ew3sn	30 m
Support practices	ESDAC	https://esdac.jrc.ec.europa.eu/content/support-practices-factor-p-factor-eu	1 km

Finally, the impact of pre-fire management practices, such as terracing, grass margins, contour farming, and stone walls on erosion was assessed by retrieving data from the European Soil Data Centre, providing comprehensive coverage for the entire Europe (Panagos et al. 2012). Brief descriptions of the dataset's characteristics (all in raster format) are presented in Table 2.

2.3 RUSLE model

The empirical model of RUSLE computes the average annual soil loss either by sheet or rill water erosion. The equation's general form involves a systematic combination of five fundamental factors (Renard et al. 1991):

$$A = R \times K \times LS \times C \times P \quad (1)$$

where A is the calculated rate of soil loss expressed in $\text{t ha}^{-1} \text{y}^{-1}$, R stands for the rainfall erosivity factor expressed in $\text{MJ mm ha h}^{-1} \text{y}^{-1}$, K is the soil erodibility factor in $\text{t ha h ha}^{-1} \text{MJ}^{-1} \text{mm}^{-1}$, S is a dimensionless factor combining the effects of slope length (L) and steepness (S), and C and P are the cover management and support practice factors, both dimensionless. The spatial resolution of the model's output is set at 30 m per pixel, a dimension deemed suitable for such applications, as highlighted by Wu et al. (2005). All layers were reprojected to the Lambert Azimuthal Equal Area (LAEA) projection (EPSG: 3035).

Subsequently, the obtained soil loss values were classified into distinct categories utilizing the classification scheme proposed by Reneuve and Galevsky (1955). This classification methodology has been proven effective in identifying areas susceptible to accelerated erosion, as Myronidis et al. (2010) demonstrated. The erosion rates were grouped in six classes according to the intensity of soil loss: Very Low ($< 5 \text{ t ha}^{-1} \text{y}^{-1}$), Low ($5\text{--}12 \text{ t ha}^{-1} \text{y}^{-1}$), Moderate ($12\text{--}50 \text{ t ha}^{-1} \text{y}^{-1}$), Severe ($50\text{--}100 \text{ t ha}^{-1} \text{y}^{-1}$), Very Severe ($100\text{--}200 \text{ t ha}^{-1} \text{y}^{-1}$), and Extreme ($> 200 \text{ t ha}^{-1} \text{y}^{-1}$).

2.3.1 Rainfall erosivity factor (R)

RUSLE's climate component R is an expression of the rainstorm kinetic energy and intensity, which influences the erosion process. The R -factor is considered of particular importance as it influences not just the detachment of the soil particles and the disintegration of soil aggregates, but also the transport of the eroded particles by runoff. The original formula introduced for the R -factor details the erosive impact of a single rainfall event by multiplying the kinetic energy of each rainstorm with its maximum intensity, during a 30 min timestep (Wischmeier 1959; Brown and Foster 1987). Following the aggregation of rainfall erosivity data from individual rainstorm events, the resulting value is then averaged over the examined period to calculate the R -factor.

Unfortunately, sub-hourly records of rainfall rates from meteorological ground stations are rarely available. As a result, simplified formulas have been created for estimating rainfall erosivity by using easily accessible monthly or daily rainfall data. The literature on methods for rainfall erosivity formulas is extensive (Nearing et al. 2017). Herein, the formula developed by Renard and Freimund (1994) was utilized, as it has been found to yield satisfactory results over forested areas in Greece (Efthimiou 2018). Subsequently, the R -factor values for both pre-and post-fire hydrological years were calculated using the following equations, where P represents the mean annual precipitations (mm):

$$R = 587.8 - 1.217 \times P + 0.004105 \times P^2 \quad \text{for } P > 850\text{mm} \quad (2)$$

$$R = 0.04830 \times P^{1.610} \quad \text{for } P > 850 \text{ mm} \quad (3)$$

2.3.2 Soil erodibility factor (K)

It expresses the soil’s exposure to erosion due to rain, is influenced by an interaction of its physicochemical, and mineralogical properties. Measuring the K-factor directly in the field is challenging and often impractical for large-scale studies. In this investigation, K was determined utilizing the equation outlined by Wischmeier and Smith (1978). All requisite data were retrieved via GEE from the SoilGrids dataset and processed within a GIS environment.

The calculation of K is expressed as follows:

$$K = \left[\left(\frac{2.1 \times 10^{-4} M^{1.14} (12 - OM) + 3.25(s - 2) + 2.5(p - 3)}{100} \right) \times 0.1317 \right] \quad (4)$$

where M is the grain size, OM is the percentage of the organic matter, s is the soil structure, and p is the soil permeability. The value of M is calculated as shown in Eq. 5 and is based on the proportions of two fractions: Ps (%) which includes the silt and the very fine sand fraction and Pc (%), which is the clay fraction:

$$M = P_s(100 - P_c) \quad (5)$$

2.3.3 Topographic factor (LS)

This factor, is influenced by geomorphology, typically encompasses slope length (L) and steepness (S). Elevated LS-factor values suggest steep relief, increasing sediment yield and erosion due to amplified runoff. To estimate the LS factor, advanced algorithms of the QGIS (v3.22) were employed, utilizing the Digital Elevation Model (DEM) as the sole input parameter. This software integrates the multiple flow algorithm, facilitating comprehensive terrain analysis.

The S-factor was derived by the formula of McCool et al. (1989), which relies on the slope gradient (θ):

$$S = \begin{cases} 10.8 \times \sin\theta + 0.03, & \text{for } \theta < 0.09 \\ 16.8 \times \sin\theta - 0.5, & \text{for } \theta > 0.09 \end{cases} \quad (6)$$

In addition, slope length (L) was determined according to the Desmet and Govers (1996) equation, yielding reliable results within complex terrain areas. This method employs the idea of unit-contributing area to regard variations in slope steepness throughout the region.

$$L = \frac{(A_{i,j-in} + D^2)^{m+1} - A_{i,j-in}^{m+1}}{D^{m+2} \times x_{i,j}^m \times 22.13^m} \quad (7)$$

where, $A_{i,j-in}$ stands for the contributing area in m^2 at the inlet of the grid cell labeled (i,j), D is the grid cell size in m, $x_{i,j}$ is a coefficient associated with aspect direction ($a_{i,j}$) of the

grid cell, calculated $x_{ij} = \sin \alpha_{ij} + \cos \alpha_{ij}$. The m coefficient is linked to the ratio β of rill to inter-rill erosion, which is dimensionless and ranges from 0 to 1.

$$m = \frac{\beta}{\beta + 1} \quad (8)$$

$$\beta = \frac{\frac{\sin \theta}{0.0896}}{[0.56 + 3 \times \sin \theta^{0.8}]} \quad (9)$$

2.3.4 Cover management factor (C)

This factor, which indicates the influence of vegetation cover, has a crucial role in shielding soil from accelerated erosion. Assessing the C-factor involves leveraging satellite-based vegetation indices.

In recent decades, the Normalized Difference Vegetation Index (NDVI) has seen widespread application. It is based on the *Red* and near-infrared (*NIR*) spectrum bands of multispectral satellite images. It is computed using a straightforward mathematical expression (Tucker 1979):

$$NDVI = \frac{NIR - Red}{NIR + Red} \quad (10)$$

To determine the C-factor, the average NDVI derived from S2-L2A images captured under both pre- and post-fire conditions was utilized (Sect. 2.2). This calculation follows a defined equation (van der Knijff et al. 2000):

$$C = \exp \left[-\alpha \left(\frac{NDVI}{\beta - NDVI} \right) \right] \quad (11)$$

In European conditions, α is set at 2 and β at 1, as illustrated in a comprehensive study spanning Europe (van der Knijff et al. 2000). Its values span from 0 to 1, while lower values donate well-conserved sites.

The process of estimating the C-factor was executed within the cloud platform. Initially, images with a cloud cover of less than 10% were meticulously selected, and a comprehensive mosaic was generated. When images overlap, the average NDVI was considered. Subsequently, utilizing the above-mentioned equation (Eq. 11), the C-factor was computed, creating an associated spatial distribution map.

2.3.5 Support practice factor (P)

The P factor is estimated considering the extent of conservation measures implemented, including strip-cropping, terracing, and contouring. Such actions aim to mitigate soil erosion caused by rainfall and runoff by redirecting runoff around the slopes, reducing erosion, or slowing down runoff to promote sediment deposition, particularly on concave slopes or through barriers like terraces or vegetation-covered strips. The P values span from 0 to 1, where lower values signify more effective erosion control measures. In this study, the values for the pre-fire condition were obtained from the previously referenced ESDAC database (see Sect. 2.2).

Table 3 Post-fire P-factor values

Slope (%)	P values
0–30	0.85
30–50	0.75
> 50	1

To model the contribution of the emergency hillslope erosion mitigation works on the erosion dynamics, the approach of Myronidis et al. (2010) was adopted. This approach aligns with the technical specifications and the guidelines set forth by the Hellenic Division of Reforestation and Mountainous Hydrology (HDRMH), aiming to safeguard soil against erosion and facilitate the restoration of the burned forest. The P-factor values were assigned to different treatment areas based on slope characteristics (Myronidis et al. 2010) (Table 3).

2.3.6 Overall workflow

The RUSLE model was applied to assess pre- and post-fire erosion rates, leveraging the advantages of cloud-computing platforms and geospatial technologies such as GIS software packages. Both dynamic factors of the RUSLE (R and C) were retrieved and processed using a significant amount of time-series data. This was facilitated by the development of appropriate code compiled in GEE. Additionally, using the platform interface, the soil erodibility (K) was calculated using the proposed equations. The support practice factor (P) in pre-fire conditions was directly derived from the ESDAC database. After implementing emergency post-fire mitigation treatments, topographic factor (LS) and P-factor values were derived by processing DEM data in the burned areas. Briefly, the flowchart of the methodological approach is shown in Fig. 2.

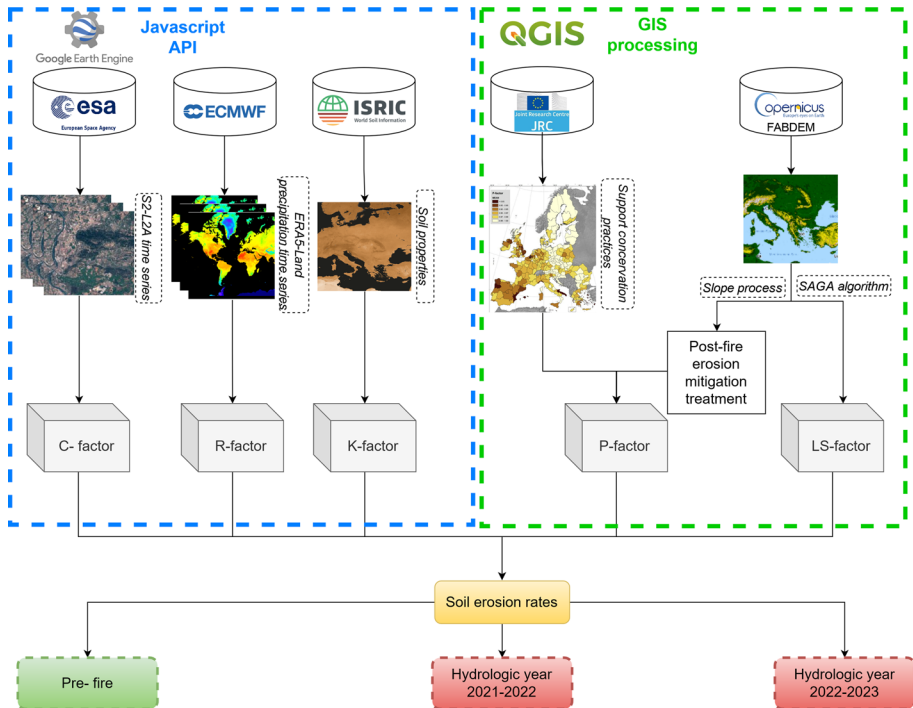


Fig. 2 Methodology flowchart

This research approach integrates open-access data into erosion modeling, facilitating the spatiotemporal monitoring of erosion rates in fire-affected landscapes. Consequently, it is highly transferable across Europe, given the extensive data coverage available. Furthermore, the robustness and efficiency of computation in GEE render the implementation of this approach feasible for large-scale assessments, including pan-European evaluations.

3 Results and discussion

The RUSLE-based modeling approach, harnessing the synergistic capabilities of the GEE platform and EO data was employed to facilitate the spatiotemporal monitoring of erosion rates in fire-affected areas. The model components were assessed for pre- and post-fire conditions in this context. The changes in vegetation conditions due to the wildfire were evaluated and the established spatio-temporal patterns of vegetation regrowth dynamics in the entire burn scar were monitored using the NDVI response. The efficiency of this index in quantifying recovery dynamics is also confirmed in the literature (Petropoulos et al. 2014; Lemsiios and Petropoulos 2024). Afterwards, the C-factor was computed directly from NDVI values. Distinct variations in the average C-factor values were evident, reflecting the extent of vegetation coverage and its associated erosion protection in the fire-affected sites before the incidents. Ancient Olympia-Gortynia exhibited the lowest average C-factor value at 0.14, indicating superior pre-fire protection from vegetation against erosion when compared with Varympompi (0.18) and Schinos (0.22). The effect of wildfires led to a notable rise in the C-factor values, with the values approximately doubling during the first hydrological year post-fire. Subsequently, these values exhibited minimal fluctuations in the second hydrological year, remaining nearly constant. Detailed regional and temporal variations in the C-factor values are presented in Fig. 3.

The R-factor values vary among the examined burned sites. They are similar in Schinos and Varympompi but approximately three times higher in Ancient Olympia–Gortynia, which promotes accelerated erosion. Moreover, a decrease in R-factor values is identified between pre- and post-wildfire conditions. Researchers have observed significant variations in erosion dynamics in the years following a fire, often attributed to notable shifts in precipitation amount and intensity (Stefanidis et al. 2002; Myronidis et al. 2010), along with changes in soil physico-chemical and hydraulic characteristics (Proutsos et al. 2023). The analytical results of the R-factor distribution at the study areas and periods are provided in

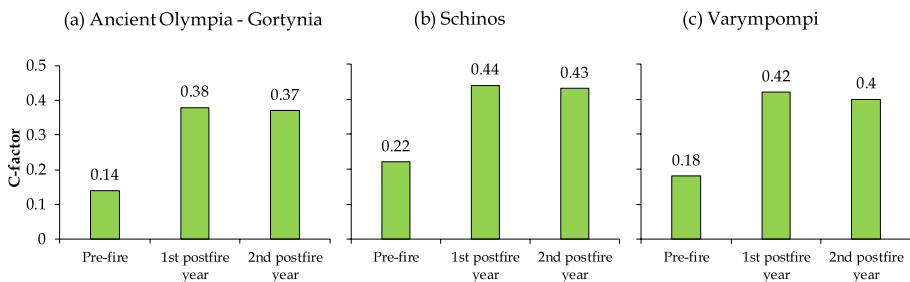


Fig. 3 C-factor average values for the pre- (2017–2020) and post-fire hydrological years (2021–2022 and 2022–2023)

Fig. 4. The RUSLE spatiotemporal assessment includes dynamic factors (C and R), enabling monitoring of erosion dynamics over time in pre- and post-fire conditions.

The ESDCA geospatial database revealed that certain land management practices were not implemented at the Varympompi and Ancient Olympia sites. This led to a P-factor value 1 in these regions before wildfire events. Following a fire, emergency hillslope post-fire erosion mitigation treatments were implemented following the technical specifications and the guidelines outlined by the Hellenic Division of Reforestation and Mountainous Hydrology (directive 86,783/7–12-1992) (Myronidis and Arabatzis 2009). Precisely, the mean P-factor across all areas was estimated to be 0.84. It is noteworthy that the P-factor not only directly impacts erosion rates but also indirectly influences C-factor values. It protects valuable forest soil against accelerated erosion and contributes to natural regeneration (Sapountzis et al. 2007). In terms of the LS factor, the highest mean values were detected in Schinos (7.95), followed by Ancient Olympia—Gortynia (5.25) and Varympompi (4.03). These findings underscore the heterogeneous nature of landscape susceptibility to erosion, highlighting the need for targeted interventions tailored to specific geographical peculiarities (Efthimiou et al. 2020b). Subsequently, the K-factor in the three sites showed similar mean values (0.029, 0.031 and 0.028 t ha h ha⁻¹ MJ⁻¹ mm⁻¹ for Ancient Olympia—Gortynia, Schinos and Varympompi, respectively). In addition, comparative studies on mathematical and machine learning models have demonstrated that machine learning can offer improved predictions for particle size distribution in fragile soils, which is crucial for accurate soil erosion assessments (Bashir et al. 2024c).

Concerning the pre-fire conditions, the mean erosion rates, as estimated by RUSLE, are characterized as very low in Varympompi (4.8 t ha⁻¹ y⁻¹) and identified as low in Ancient Olympia—Gortynia (9.8 t ha⁻¹ y⁻¹) and Schinos (11.6 t ha⁻¹ y⁻¹), based on the classification scheme of Reneuve and Galevsky (1955), already given in the previous sections. However, it is notable that such values exceed the pan-European average (Panagos et al. 2015), which stands at 2.46 t ha⁻¹ y⁻¹. The rationale for these disparities lies in the observation that EU Member States in the Mediterranean account for 67% of the overall EU soil loss, primarily due to elevated levels of rainfall erosivity (Panagos et al. 2015).

After wildfires, the absence of vegetation coverage leads to a significant increase in potential erosion rates in affected areas despite the implementation of emergency post-fire erosion control treatments (Shakesby 2011). For instance, during the first hydrological year, postfire mean erosion rates were increased to 118.3, 72.2 and 28.8 t ha⁻¹ y⁻¹, in Ancient Olympia—Gortynia, Schinos, and Varympompi respectively, being much lower during the pre-fire period. Figure 5 graphically depicts the temporal changes in erosion

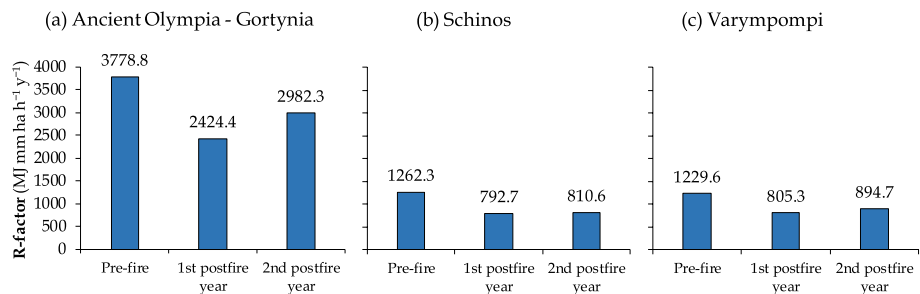


Fig. 4 R-factor average values for the pre- (2017–2020) and post-fire hydrological years (2021–2022 and 2022–2023)

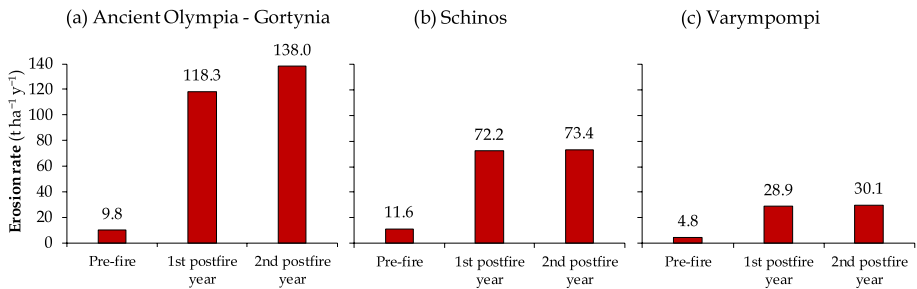


Fig. 5 Average erosion rates for the pre- (2017–2020) and post-fire hydrological years (2021–2022 and 2022–2023)

rates at the burned sites during the pre-fire period (2017–2020) and the two post-fire hydrological years (2021–2022 and 2022–2023).

These results align with similar studies in the Mediterranean basin, indicating that erosion rates can be up to ten times higher in the post-fire periods (Mallinis et al. 2009; Vieira et al. 2023). In the second hydrological year, erosion rates remained nearly stable as vegetation slightly recovered and recorded precipitation was marginally higher. This observation underscores the findings of the pan-European study of Vieira et al. (2023), which supports the necessity for a five-year monitoring framework in fire-affected areas to comprehensively assess and manage the long-term erosion dynamics due to vegetation's slow and incomplete recovery. The spatiotemporal changes in erosion rates in the examined burned sites are shown in Fig. 6.

RUSLE was applied to scenarios with and without restoration treatments to evaluate the impact of emergency post-fire hillslope restoration works on erosion dynamics. Specifically, the model quantifies the effects of these treatments on erosion potential by assigning values to the model's support practice factor (P-factor), as described in Table 3. Overall, an estimated reduction in soil loss rate of about 18% was observed due to the implementation of the restoration works in the study areas (Fig. 7). Notably, the erosion regulation services provided by these treatments are exceptionally effective, leading to an average reduction of erosion rates by 23, 12 and 6 $\text{t ha}^{-1} \text{y}^{-1}$ in Ancient Olympia—Gortynia, Schinos, Varympompi, respectively, during the two years following the wildfires. These reductions are significant compared to Europe's average soil formation rate (Verheijen et al. 2009), which is only 1.4 $\text{t ha}^{-1} \text{y}^{-1}$.

Retaining soil through emergency post-fire treatments is crucial for protecting the valuable, fertile forest soils essential for vegetation regeneration and ecosystem recovery (Sapountzis et al. 2007). They are also considered their positive impact on precipitation infiltration (Proutsos et al. 2023). These treatments are essential in Mediterranean regions, particularly Greece, where forest soils in the hilly and mountainous areas are mainly shallow (Nakos 1991). Additionally, these measures safeguard the lowland areas and plain stream beds from sedimentation during high-flow events, which can lead to flooding (Stefanidis et al. 2012).

The coupling of the RUSLE model with GEE cloud-computing services, applied in this study, can be an effective monitoring tool for the erosion processes in the post-fire environment, as also demonstrated by recent studies (Stefanidis et al. 2022; Demir and Dursum 2024; Ouallali et al. 2024). It provides access to an extensive list of long-term Earth Observation products and delivers unparalleled computational power recent advancements in machine learning algorithms have further enhanced the ability to spatially map

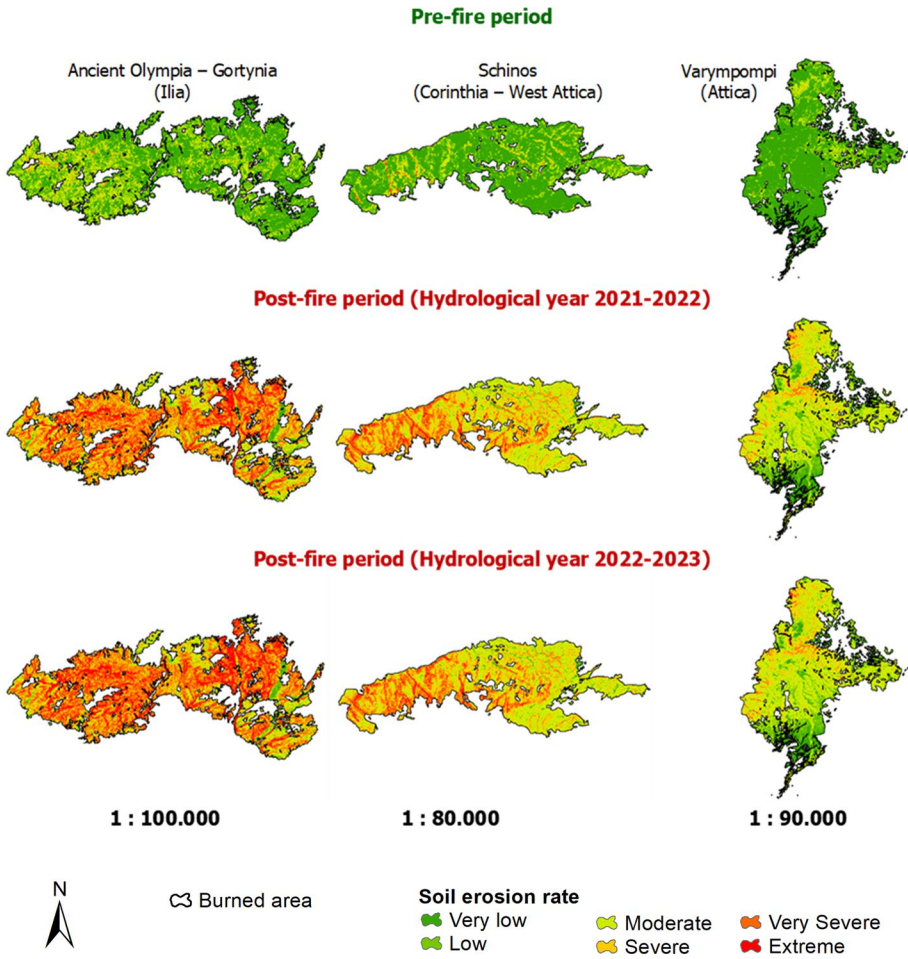


Fig. 6 Spatiotemporal distribution of erosion rates in the burned areas

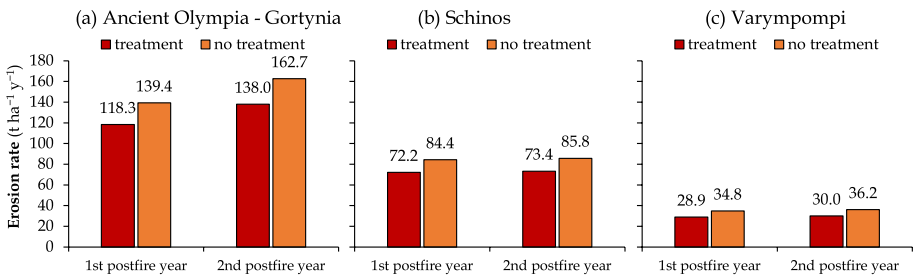


Fig. 7 Effects of postfire treatment on erosion rates during the postfire hydrological years

multi-hazard land management in sparsely vegetated watersheds. The integration of these advanced techniques with traditional modeling approaches can significantly improve the accuracy of erosion rate predictions and hazard assessments (Bammou et al. 2024b). Moreover, the RUSLE model effectively estimates soil erosion rates in Mediterranean landscapes, particularly in identifying areas at high risk for erosion (Napoli et al. 2016; Eftimiou 2016; Rellini et al. 2019). Therefore, it can be a valuable tool for stakeholders and policymakers in spatial planning and scheduling restoration projects. It also aids in monitoring and evaluating the effectiveness of treatments in data-scarce regions and supports timely large-scale assessments. The findings align with those of Stefanidis et al. (2024), who emphasized the importance of soil conservation ecosystem services from peri-urban watersheds in sustainable land management and urban planning at national scale.

It should be mentioned, however, that despite its practical utility, the RUSLE model exhibits several limitations (Kumar et al. 2022). This simplifies the extremely complicated and non-linear process of soil erosion into a trivial multiplication of the independent factors of precipitation, soil properties, landscape features, vegetation, and erosion management techniques (Lopes et al. 2021). Critical processes such as sediment transport, deposition, as well as routing within hydrographic networks, are not considered. Furthermore, the model's application is primarily confined to estimating sheet and rill erosion and does not extend to gully or stream bank erosion. Its performance across large spatial scales where environmental conditions vary widely can also be controversial. Additionally, while RUSLE may provide less accurate predictions for individual flood events due to random fluctuations, its accuracy improves over longer time scales, where variations are averaged (Eftimiou et al. 2014).

Considering these constraints, it is crucial to validate the RUSLE model for practical applications. The ongoing research plans to compare the soil retained from constructed erosion control works with actual field measurements taken during the examined period. This analysis will critically assess the model's accuracy and effectiveness, and the results will be discussed in a forthcoming study.

4 Conclusion

This research marks a major advancement in the ongoing observation of soil erosion following wildfires within Mediterranean ecosystems using Earth Observation (EO) data integrated with cloud computing technologies. Through the implementation of the RUSLE in conjunction with the GEE, the impacts of wildfires on soil erosion dynamics can be precisely quantified across various landscapes in Greece.

Our findings revealed dramatic increases in erosion rates immediately following wildfire events, which were significantly mitigated by implementing emergency post-fire treatments. Using high-resolution EO data allowed for a nuanced understanding of the spatial variations in erosion, linking them effectively to both biotic recovery and abiotic changes in the landscape. This approach provided a rapid assessment capability and enhanced the accuracy of predicting areas at risk, thereby facilitating more targeted land management strategies.

The implications of our research extend beyond the academic sphere, offering vital insights for policymakers and land management officials. By providing a method incorporating historical data and real-time analysis, this study supports the development of adaptive management strategies that can respond to the immediate effects of wildfires.

Moreover, our work underscores the importance of integrating technological advancements with traditional conservation practices to enhance ecosystem resilience and recovery post-disturbance.

Future studies will aim to confirm the findings of the RUSLE model and apply this approach to other regions around the globe that are susceptible to wildfires, improving the model's predictive capabilities with additional variables, and exploring the long-term ecological impacts of soil erosion. By continuing to refine these approaches, we can better prepare and respond to the increasing challenges posed by climate change and its impact on wildfire frequency and intensity. This study advances our understanding of post-fire dynamics in Mediterranean landscapes and sets a precedent for integrating technological innovations into environmental management and policy formulation, aiming for a sustainable balance between human needs and ecosystem health.

Author contributions Conceptualization: Stefanos P. Stefanidis, Nikolaos D. Proutsos; Methodology: Stefanos P. Stefanidis, Nikolaos D. Proutsos, Athanassios Bourletsikas, Dimitris Tigkas; Formal analysis and investigation: Stefanos P. Stefanidis, Nikolaos D. Proutsos, Alexandra D. Solomou; Writing—original draft preparation: Stefanos P. Stefanidis, Nikolaos D. Proutsos, Dimitris Tigkas, Shuraik Kader, Panagiotis Michopoulos; Writing—review and editing: Stefanos P. Stefanidis, Nikolaos D. Proutsos, Dimitris Tigkas, Velibor Spalevic, Alexandra D. Solomou, Shuraik Kader; Funding acquisition: Nikolaos D. Proutsos; Resources: Stefanos P. Stefanidis, Nikolaos D. Proutsos, Shuraik Kader; Supervision: Nikolaos D. Proutsos. All authors read and approved the final manuscript.

Funding This research was financially supported by the Hellenic Green Fund (Grant number 21SYMV008996029 2021–07-28). Research Project: MoRe Forests “MONitoring the impact of REstoration works in the post fire Forest environment in Greece”.

Data availability The datasets generated during and/or analyzed during the current study are available from the corresponding author on reasonable request.

Declarations

Conflict of interest The authors have no relevant financial or non-financial interests to disclose.

References

- Akin ID, Akinleye TO, Robichaud PR (2023) Changes in soil properties over time after a wildfire and implications to slope stability. *J Geotech Geoenviron Eng* 149(7):04023045. <https://doi.org/10.1061/JGGEFK.GTENG-11348>
- Alewell C, Borrelli P, Meusburger K, Panagos P (2019) Using the USLE: chances, challenges and limitations of soil erosion modelling. *Int Soil Water Conserv Res* 7(3):203–225. <https://doi.org/10.1016/j.iswcr.2019.05.004>
- Alexandridis V, Stefanidis S, Dafis S (2023) Evaluation of ERA5 and ERA5-land reanalysis precipitation data with rain gauge observations in Greece. *Environ Sci Proceed* 26(1):104. <https://doi.org/10.3390/envirosci2023026104>
- Bammou Y, Benzougagh B, Abdessalam O, Brahim I, Kader S, Spalevic V, Ercişli S (2024) Machine learning models for gully erosion susceptibility assessment in the tensift catchment, haouz plain, morocco for sustainable development. *J Afr Earth Sci* 213:105229. <https://doi.org/10.1016/j.jafrearsci.2024.105229>
- Bammou Y, Benzougagh B, Igmoullan B, Kader S, Ouallali A, Spalevic V, Kuriqi A (2024) Spatial mapping for multi-hazard land management in sparsely vegetated watersheds using machine learning algorithms. *Environ Earth Sci* 83(15):447. <https://doi.org/10.1007/s12665-024-11741-9>

- Bashir O, Bangroo SA, Shafai SS, Senesi N, Kader S, Alamri S (2024a) Geostatistical modeling approach for studying total soil nitrogen and phosphorus under various land uses of North-Western Himalayas. *Eco Inform* 80:102520. <https://doi.org/10.1016/j.ecoinf.2024.102520>
- Bashir O, Bangroo SA, Shafai SS, Senesi N, Naikoo NB, Kader S, Jaufer L (2024b) Unlocking the potential of soil potassium: geostatistical approaches for understanding spatial variations in North Western Himalayas. *Eco Inform* 81:102592. <https://doi.org/10.1016/j.ecoinf.2024.102592>
- Bashir O, Bangroo SA, Shafai SS, Shah TI, Kader S, Jaufer L, Hysa A (2024) Mathematical vs. machine learning models for particle size distribution in fragile soils of North-Western Himalayas. *J Soils Sedim* 24:2294–2308. <https://doi.org/10.1007/s11368-024-03820-y>
- Bombino G, Barbaro G, Pérez-Cutillas P, D'Agostino D, Denisi P, Foti G, Zimbone SM (2023) Use of logs downed by wildfires as erosion barriers to encourage forest auto-regeneration: a case study in Calabria Italy. *Water* 15(13):2378. <https://doi.org/10.3390/w15132378>
- Bond WJ, Woodward FI, Midgley GF (2005) The global distribution of ecosystems in a world without fire. *New Phytol* 165(2):525–538. <https://doi.org/10.1111/j.1469-8137.2004.01252.x>
- Brovelli MA, Sun Y, Yordanov V (2020) Monitoring forest change in the amazon using multi-temporal remote sensing data and machine learning classification on Google earth engine. *ISPRS Int J Geo Inf* 9(10):580
- Brown LC, Foster GR (1987) Storm erosivity using idealized intensity distributions. *Trans ASAE* 30(2):379–0386
- Carrión JS, Sánchez-Gómez P, Mota JF, Yll R, Chain C (2003) Holocene vegetation dynamics, fire and grazing in the Sierra de Gádor, southern Spain. *Holocene* 13(6):839–849. <https://doi.org/10.1191/0959683603hl662rp>
- Demir S, Dursun İ (2024) Assessment of pre-and post-fire erosion using the RUSLE equation in a watershed affected by the forest fire on Google earth engine: the study of Manavgat River Basin. *Nat Hazards*. <https://doi.org/10.1007/s11069-023-06291-5>
- Desmet PJ, Govers G (1996) A GIS procedure for automatically calculating the USLE LS factor on topographically complex landscape units. *J Soil Water Conserv* 51(5):427–433
- Duarte E, Obrist-Farner J, Correa-Metrio A, Steinman BA (2021) A progressively wetter early through middle Holocene climate in the eastern lowlands of Guatemala. *Earth Planet Sci Lett* 561:116807. <https://doi.org/10.3390/land10060554>
- Efthimiou N (2016) Performance of the RUSLE in Mediterranean mountainous catchments. *Environ Process* 3:1001–1019. <https://doi.org/10.1007/s40710-016-0174-y>
- Efthimiou N (2018) Evaluating the performance of different empirical rainfall erosivity (R) factor formulas using sediment yield measurements. *CATENA* 169:195–208. <https://doi.org/10.1016/j.catena.2018.05.037>
- Efthimiou N, Lykoudi E, Karavitis C (2014) Soil erosion assessment using the RUSLE model and GIS. *Europ Water* 47:15–30
- Efthimiou N, Psomiadis E, Panagos P (2020a) Fire severity and soil erosion susceptibility mapping using multi-temporal earth observation data: the case of mati fatal wildfire in Eastern Attica. *Greece Catena* 187:104320. <https://doi.org/10.1016/j.catena.2019.104320>
- Efthimiou N, Lykoudi E, Psomiadis E (2020b) Inherent relationship of the USLE, RUSLE topographic factor algorithms and its impact on soil erosion modelling. *Hydrol Sci J* 65(11):1879–1893
- Elnashar A, Zeng H, Wu B, Fenta AA, Nabil M, Duerler R (2021) Soil erosion assessment in the Blue Nile Basin driven by a novel RUSLE-GEE framework. *Sci Total Environ* 793:148466. <https://doi.org/10.1016/j.scitotenv.2021.148466>
- Girona-García A, Vieira DC, Silva J, Fernández C, Robichaud PR, Keizer JJ (2021) Effectiveness of post-fire soil erosion mitigation treatments: a systematic review and meta-analysis. *Earth Sci Rev* 217:103611. <https://doi.org/10.1016/j.earscirev.2021.103611>
- Gomis-Cebolla J, Rattayova V, Salazar-Galán S, Francés F (2023) Evaluation of ERA5 and ERA5-Land reanalysis precipitation datasets over Spain (1951–2020). *Atmos Res* 284:106606. <https://doi.org/10.1016/j.atmosres.2023.106606>
- Gorelick N, Hancher M, Dixon M, Ilyushchenko S, Thau D, Moore R (2017) Google earth engine: planetary-scale geospatial analysis for everyone. *Remote Sens Environ* 202:18–27. <https://doi.org/10.1016/j.rse.2017.06.031>
- Hawker L, Uhe P, Paulo L, Sosa J, Savage J, Sampson C, Neal J (2022) A 30 m global map of elevation with forests and buildings removed. *Environ Res Lett* 17(2):024016. <https://doi.org/10.1088/1748-9326/ac4d4f>
- Hengl T, Mendes de Jesus J, Heuvelink GBM, Ruiperez Gonzalez M et al (2017) SoilGrids250m: Global gridded soil information based on machine learning. *PLoS ONE* 12(2):e0169748

- Immitzer M, Vuolo F, Atzberger C (2016) First experience with Sentinel-2 data for crop and tree species classifications in central Europe. *Remote Sens* 8(3):166. <https://doi.org/10.3390/rs8030166>
- Islam F, Ahmad MN, Janjuhah HT, Ullah M, Islam IU, Kontakiotis G, Skilodimou HD, Bathrellos GD (2022) Modelling and mapping of soil erosion susceptibility of Murree, sub-Himalayas using GIS and RS based model. *Appl Sci Basel* 12(23):12211. <https://doi.org/10.3390/app122312211>
- Karamesouti M, Petropoulos GP, Papanikolaou ID, Kairis O, Kosmas K (2016) Erosion rate predictions from PESERA and RUSLE at a Mediterranean site before and after a wildfire: comparison and implications. *Geoderma* 261:44–58. <https://doi.org/10.1016/j.geoderma.2015.06.025>
- Kumar M, Sahu AP, Sahoo N, Dash SS, Raul SK, Panigrahi B (2022) Global-scale application of the RUSLE model: a comprehensive review. *Hydrol Sci J* 67(5):806–830. <https://doi.org/10.1080/02626667.2021.2020277>
- Lanorte A, Cillis G, Calamita G, Nolè G, Pilogallo A, Tucci B, De Santis F (2019) Integrated approach of RUSLE, GIS and ESA Sentinel-2 satellite data for post-fire soil erosion assessment in Basilicata region (Southern Italy). *Geomat Nat Haz Risk* 10(1):1563–1595. <https://doi.org/10.1080/19475705.2019.1578271>
- Lecina-Diaz J, Martínez-Vilalta J, Alvarez A, Vayreda J, Retana J (2021) Assessing the risk of losing forest ecosystem services due to wildfires. *Ecosystems* 24:1–15. <https://doi.org/10.1007/s10021-021-00611-1>
- Lemesios I, Petropoulos GP (2024) Vegetation regeneration dynamics of a natural mediterranean ecosystem following a wildfire exploiting the LANDSAT archive, google earth engine and geospatial analysis techniques. *Remote Sens Appl: Soc Environ* 34:101153
- Lopes AR, Girona-García A, Corticeiro S, Martins R, Keizer JJ, Vieira DCS (2021) What is wrong with post-fire soil erosion modelling? A meta-analysis on current approaches, research gaps, and future directions. *Earth Surf Proc Land* 46(1):205–219. <https://doi.org/10.1002/esp.5020>
- Mallinis G, Maris F, Kalinderis I, Koutsias N (2009) Assessment of post-fire soil erosion risk in fire-affected watersheds using remote sensing and GIS. *GISci Remote Sens* 46(4):388–410
- Mallinis G, Gitas IZ, Tasionas G, Maris F (2016) Multitemporal monitoring of land degradation risk due to soil loss in a fire-prone mediterranean landscape using multi-decadal Landsat imagery. *Water Resour Manage* 30:1255–1269. <https://doi.org/10.1007/s11269-016-1224-y>
- Marsh CB, Harder P, Pomeroy JW (2023) Validation of FABDEM, a global bare-earth elevation model, against UAV-lidar derived elevation in a complex forested mountain catchment. *Environ Res Commun* 5(3):031009. <https://doi.org/10.1088/2515-7620/acc56>
- McCool DK, Foster GR, Mutchler CK, Meyer LD (1989) Revised slope length factor for the universal soil loss equation. *Trans ASAE* 30:1387–1396
- Michopoulos P, Proutos ND, Solomou AD, Bourletsikas A, Tsilikounas S, Louka V, Lattas P, Kalliris P, Blanos G (2023) Effects of restoration works on soil properties of burned forest areas. In: Proceedings of the 3rd Mediterranean Geosciences Union Annual Meeting MedGU 2023, 26–30 November 2023, Istanbul, Türkiye. In: Springer series Advances in Science, Technology and Innovation (ASTI) (in press, indexed in Scopus)
- Mitsopoulos I, Mallinis G, Dimitrakopoulos A, Xanthopoulos G, Eftychidis G, Goldammer JG (2020) Vulnerability of peri-urban and residential areas to landscape fires in Greece: Evidence by wildland-urban interface data. *Data Brief* 31:106025. <https://doi.org/10.1016/j.dib.2020.106025>
- Moody JA, Shakesby RA, Robichaud PR, Cannon SH, Martin DA (2013) Current research issues related to post-wildfire runoff and erosion processes. *Earth Sci Rev* 122:10–37. <https://doi.org/10.1016/j.earscirev.2013.03.004>
- Myronidis D, Arabatzis G (2009) Evaluation of greek post-fire erosion mitigation policy through spatial analysis. *Pol J Environ Stud* 18(5):865–872
- Myronidis DI, Emmanouloudis DA, Mitsopoulos IA, Riggos EE (2010) Soil erosion potential after fire and rehabilitation treatments in Greece. *Environ Model Assess* 15:239–250. <https://doi.org/10.1007/s10666-009-9199-1>
- Nakos G (1991) Classification, mapping and assessment of lands: technical instructions. Institute of Institute of Mediterranean Forest Ecosystems, In Greek
- Napoli M, Cecchi S, Orlandini S, Mugnai G, Zanchi CA (2016) Simulation of field-measured soil loss in Mediterranean hilly areas (Chianti, Italy) with RUSLE. *Catena* 145:246–256. <https://doi.org/10.1016/j.catena.2016.06.018>
- Nearing MA, Yin SQ, Borrelli P, Polyakov VO (2017) Rainfall erosivity: an historical review. *Catena* 157:357–362. <https://doi.org/10.1016/j.catena.2017.06.004>
- Nourizadeh M, Naghavi H, Omidvar E (2024) The effect of land use and land cover changes on soil erosion in semi-arid areas using cloud-based google earth engine platform and GIS-based RUSLE model. *Nat Hazards* 120:2499–2527. <https://doi.org/10.1007/s11069-023-06291-5>

- Ouallali A, Kader S, Bammou Y, Aqnouy M, Courba S, Beroho M, Hysa A (2024) Assessment of the erosion and outflow intensity in the rif region under different land use and land cover scenarios. *Land*. <https://doi.org/10.3390/land13020141>
- Panagos P, Van Liedekerke M, Jones A, Montanarella L (2012) European soil data centre: response to European policy support and public data requirements. *Land Use Policy* 29(2):329–338. <https://doi.org/10.1016/j.landusepol.2011.07.003>
- Panagos P, Borrelli P, Poesen J, Ballabio C, Lugato E, Meusburger K, Montanarella L, Alewell C (2015) The new assessment of soil loss by water erosion in Europe. *Environ Sci Policy* 54:438–447. <https://doi.org/10.1016/j.envsci.2015.08.012>
- Pausas JG, Keeley JE (2021) Wildfires and global change. *Front Ecol Environ* 19(7):387–395. <https://doi.org/10.1002/fee.2359>
- Pausas JG, Ribeiro E (2017) Fire and plant diversity at the global scale. *Glob Ecol Biogeogr* 26(8):889–897. <https://doi.org/10.1111/geb.12596>
- Pausas JG, Ribeiro E, Vallejo R (2004) Post-fire regeneration variability of *Pinus halepensis* in the eastern Iberian Peninsula. *For Ecol Manage* 203(1–3):251–259. <https://doi.org/10.1016/j.foreco.2004.07.061>
- Pausas JG, Llovet J, Rodrigo A, Vallejo R (2008) Are wildfires a disaster in the Mediterranean basin?—A review. *Int J Wildland Fire* 17(6):713–723. <https://doi.org/10.1071/WF07151>
- Petropoulos GP, Griffiths HM, Kalivas DP (2014) Quantifying spatial and temporal vegetation recovery dynamics following a wildfire event in a Mediterranean landscape using EO data and GIS. *Appl Geogr* 50:120–131. <https://doi.org/10.1016/j.apgeog.2014.02.006>
- Proutsos ND, Tsiros IX, Nastos P, Tsaousidis A (2021) A note on some uncertainties associated with Thornthwaite’s aridity index introduced by using different potential evapotranspiration methods. *Atmos Res* 260:105727. <https://doi.org/10.1016/j.atmosres.2021.105727>
- Proutsos ND, Solomou AD, Tigkas D (2022) Decadal variation of aridity and water balance attributes at the urban and peri-urban environment of Attica-Greece. In: proceedings of the 10th international conference on information and communication technologies in agriculture, food and environment, HAICTA 2022, September 22–25, 2022, Athens, Greece, CEUR Workshop Proceedings (CEUR-WS.org), Vol. 3293, pp. 472–477
- Proutsos ND, Solomou AD, Michopoulos P, Bourletsikas A, Tsilikounas S, Louka V, Lattas P, Kalliris P (2023) Soil Optical and Hydraulic Properties of Burnt Forest Areas in Greece after the Implementation of Postfire Restoration Works—Preliminary Results. *Environmental Sciences Proceedings (Proceedings of 16th International Conference on Meteorology, Climatology and Atmospheric Physics—COMECAP 2023)*, Athens, Greece, 25–29 September 2023 26(1), 27 <https://doi.org/10.3390/environsciproc2023026027>
- Rellini I, Scopesi C, Olivari S, Firpo M, Maerker M (2019) Assessment of soil erosion risk in a typical Mediterranean environment using a high resolution RUSLE approach (Portofino promontory, NW-Italy). *J Maps* 15(2):356–362
- Renard KG, Freimund JR (1994) Using monthly precipitation data to estimate the R-factor in the revised USLE. *J Hydrol* 157(1–4):287–306. [https://doi.org/10.1016/0022-1694\(94\)90110-4](https://doi.org/10.1016/0022-1694(94)90110-4)
- Renard KG, Foster GR, Weesies GA, Porter JP (1991) RUSLE: revised universal soil loss equation. *J Soil Water Conserv* 46(1):30–33
- Reneuve P, Galevski M (1955) La corrélation entre les pluies torrentielles et l’intensité de l’érosion (d’après les observations faites dans un périmètre torrentiel)-Avant-propos. *Annales De L’école Nationale Des Eaux Et Forêts Et De La Station De Recherches Et Expériences Forestières* 14(2):379–428
- Robichaud PR (2005) Measurement of post-fire hillslope erosion to evaluate and model rehabilitation treatment effectiveness and recovery. *Int J Wildland Fire* 14(4):475–485. <https://doi.org/10.1071/WF05031>
- Robichaud PR, Ashmun LE (2012) Tools to aid post-wildfire assessment and erosion-mitigation treatment decisions. *Int J Wildland Fire* 22(1):95–105. <https://doi.org/10.1071/WF11162>
- Sadkaoui D, Brahim B, Kader S, Agharroud K, Mihraje AI, Aluni K, Sestras P (2024) Evaluation of tectonic activity using morphometric indices: study of the case of taïliloute ridge (middle-Atlas region, Morocco). *J Afr Earth Sci* 213:105219. <https://doi.org/10.1016/j.jafrearsci.2024.105219>
- Sapountzis MA, Efthimiou GS, Stefanidis PS (2007) The contribution of agrotechnical works following a fire to the protection of forest soils and the regeneration of natural forest. In eco-and ground bio-engineering: the use of vegetation to improve slope stability: proceedings of the first international conference on eco-engineering 13–17 September 2004 (pp. 353–359). Springer Netherlands. https://doi.org/10.1007/978-1-4020-5593-5_35
- Sestras P, Mircea S, Roșca S, Bilașco Ș, Sălăgean T, Dragomir LO, Kader S (2023) GIS based soil erosion assessment using the USLE model for efficient land management: a case study in an area with

- diverse pedo-geomorphological and bioclimatic characteristics. *Not Bot Horti Agrobot Cluj-Napoca* 51(3):13263–13263
- Shakesby RA (2011) Post-wildfire soil erosion in the Mediterranean: review and future research directions. *Earth Sci Rev* 105(3–4):71–100. <https://doi.org/10.1016/j.earscirev.2011.01.001>
- Shakesby RA, Doerr SH (2006) Wildfire as a hydrological and geomorphological agent. *Earth Sci Rev* 74(3–4):269–307. <https://doi.org/10.1016/j.earscirev.2005.10.006>
- Silvestro R, Saulino L, Cavallo C, Allevato E, Pindozi S, Cervelli E, Conti P, Mazzoleni S, Saracino A (2021) The footprint of wildfires on mediterranean forest ecosystem services in vesuvius national park. *Fire* 4(4):95. <https://doi.org/10.3390/fire4040095>
- Skilodimou HD, Bathrellos GD (2021) Natural and technological hazards in Urban areas: assessment. *Plan Solut Sustain* 13(15):8301. <https://doi.org/10.3390/su13158301>
- Solomou AD, Proutsos ND, Michopoulos P, Bourletsikas A, Tsilikounas S, Louka V, Lattas P, Kalliris P, Blanos G (2023) Short-term vascular plant biodiversity assessment in burned and restored forest areas of Greece. In: Proceedings of the 3rd mediterranean geosciences union annual meeting MedGU 2023, 26–30 November 2023, Istanbul, Türkiye. In: Springer series Advances in Science, Technology & Innovation (ASTI) (in press)
- Spanos IA, Daskalaku EN, Thanos CA (2000) Postfire, natural regeneration of *Pinus brutia* forests in Thasos island. *Greece Acta Oecologica* 21(1):13–20. [https://doi.org/10.1016/S1146-609X\(00\)00107-7](https://doi.org/10.1016/S1146-609X(00)00107-7)
- Spigel KM, Robichaud PR (2007) First-year post-fire erosion rates in Bitterroot National Forest Montana. *Hydrol Process Int J* 21(8):998–1005. <https://doi.org/10.1002/hyp.6295>
- Stefanidis P, Sapountzis M, Stathis D (2002) Sheet erosion after fire at the urban forest of Thessaloniki (Northern Greece). *Silva Balcanica* 2:65–77
- Stefanidis P, Sapountzis M, Tziafani F, Stefanidis S (2012) Torrent control works at the region of Peloponnese (Greece) after forest fire of 2007. In: Zlatic M, Kostadinov S (eds) Challenges: sustainable land management—climate change. Catena Verlag, Reiskirchen, Germany, pp 148–155
- Stefanidis S, Alexandridis V, Mallinis G (2022) A cloud-based mapping approach for assessing spatiotemporal changes in erosion dynamics due to biotic and abiotic disturbances in a Mediterranean Peri-Urban forest. *CATENA* 218:106564. <https://doi.org/10.1016/j.catena.2022.106564>
- Stefanidis S, Proutsos N, Alexandridis V, Mallinis G (2024) Ecosystem services supply from Peri-Urban watersheds in Greece: soil conservation and water retention. *Land* 13(6):765. <https://doi.org/10.3390/land13060765>
- Tamiminia H, Salehi B, Mahdianpari M, Quackenbush L, Adeli S, Brisco B (2020) Google earth engine for geo-big data applications: a meta-analysis and systematic review. *ISPRS J Photogramm Remote Sens* 164:152–170. <https://doi.org/10.1016/j.isprsjprs.2020.04.001>
- Thornthwaite CW (1948) An approach toward a rational classification of climate. *Geogr Rev* 38(1):55–94. <https://doi.org/10.2307/210739>
- Tsiros IX, Nastos P, Proutsos ND, Tsaousidis A (2020) Variability of the aridity index and related drought parameters in Greece using climatological data over the last century (1900–1997). *Atmos Res* 240:104914. <https://doi.org/10.1016/j.atmosres.2020.104914>
- Tucker CJ (1979) Red and photographic infrared linear combinations for monitoring vegetation. *Remote Sens Environ* 8(2):127–150. [https://doi.org/10.1016/0034-4257\(79\)90013-0](https://doi.org/10.1016/0034-4257(79)90013-0)
- UNEP (1992) World atlas of desertification. United Nations Environment Program, London
- Valkanou K, Karymbalis E, Bathrellos GD, Skilodimou HD, Tsanakas K, Papanastassiou D, Gaki-Papanastassiou K (2022) soil loss potential assessment for natural and post-fire condition in evia Island. *Greece Geosci* 12(10):367. <https://doi.org/10.3390/geosciences12100367>
- Van der Knijff JM, Jones RJA, Montanarella L (2000) Soil erosion risk assessment in Europe, EUR 19044 EN. Office for official publications of the European communities, Luxembourg, p 34
- Vanmaercke M, Poesen J, Radoane M, Govers G, Ocakoglu F, Arabkhedri M (2012) How long should we measure? An exploration of factors controlling the inter-annual variation of catchment sediment yield. *J Soils Sediments* 12:603–619. <https://doi.org/10.1007/s11368-012-0475-3>
- Verde N, Kokkoris IP, Georgiadis C, Kaimaris D, Dimopoulos P, Mitsopoulos I, Mallinis G (2020) National scale land cover classification for ecosystem services mapping and assessment, using multitemporal copernicus EO data and google earth engine. *Remote Sens* 12(20):3303. <https://doi.org/10.3390/rs12203303>
- Verheijen FG, Jones RJ, Rickson RJ, Smith CJ (2009) Tolerable versus actual soil erosion rates in Europe. *Earth Sci Rev* 94(1–4):23–38. <https://doi.org/10.1016/j.earscirev.2009.02.003>
- Vieira DCS, Borrelli P, Jahaniannard D, Benali A, Scarpa S, Panagos P (2023) Wildfires in Europe: burned soils require attention. *Environ Res* 217:114936. <https://doi.org/10.1016/j.envres.2022.114936>

- Vilar L, Camia A, San-Miguel-Ayanz J, Martín MP (2016) Modeling temporal changes in human-caused wildfires in Mediterranean Europe based on Land Use-Land Cover interfaces. *For Ecol Manage* 378:68–78. <https://doi.org/10.1016/j.foreco.2016.07.020>
- Wischmeier WH (1959) A rainfall erosion index for a universal soil-loss equation. *Soil Sci Soc Am J* 23(3):246–249
- Wischmeier WH, Smith DD (1978) Predicting rainfall erosion losses: a guide to conservation planning (No. 537). Department of Agriculture, Science and Education Administration
- Wu S, Li J, Huang G (2005) An evaluation of grid size uncertainty in empirical soil loss modeling with digital elevation models. *Environ Model Assess* 10:33–42. <https://doi.org/10.1007/s10666-004-6595-4>

Publisher's Note Springer Nature remains neutral with regard to jurisdictional claims in published maps and institutional affiliations.

Springer Nature or its licensor (e.g. a society or other partner) holds exclusive rights to this article under a publishing agreement with the author(s) or other rightsholder(s); author self-archiving of the accepted manuscript version of this article is solely governed by the terms of such publishing agreement and applicable law.

Authors and Affiliations

Stefanos P. Stefanidis¹  · **Nikolaos D. Proutsos**² · **Alexandra D. Solomou**² · **Panagiotis Michopoulos**² · **Athanassios Bourletsikas**² · **Dimitris Tigkas**³ · **Velibor Spalevic**⁴ · **Shuraik Kader**⁵

✉ Stefanos P. Stefanidis
sstefanidis@elgo.gr

Nikolaos D. Proutsos
np@fria.gr

Alexandra D. Solomou
asolomou@elgo.gr

Panagiotis Michopoulos
mipa@fria.gr

Athanassios Bourletsikas
abourletsikas@elgo.gr

Dimitris Tigkas
ditigas@mail.ntua.gr

Velibor Spalevic
velibors@ucg.ac.me

Shuraik Kader
s.mohamedabdulkader@griffith.edu.au; shuraik.mohamedabdulkader@griffithuni.edu.au;
shuraik10@gmail.com

¹ Forest Research Institute, Hellenic Agricultural Organization—DIMITRA, 57006 Vassilika, Thessaloniki, Greece

² Institute of Mediterranean Forest Ecosystems, Hellenic Agricultural Organization—DIMITRA, Terma Alkmanos, 11528 Athens, Greece

³ Centre for the Assessment of Natural Hazards and Proactive Planning and Laboratory of Reclamation Works and Water Resources Management, National Technical University of Athens, 15780 Athens, Greece

⁴ Biotechnical Faculty, University of Montenegro, 81000 Podgorica, Montenegro

⁵ School of Engineering and Built Environment, Griffith University, Nathan, QLD 4111, Australia